DOI: 10.1002/ejic.201001359

A Polymorphic Platinum(II) Complex: Yellow, Red, and Green Polymorphs and X-ray Crystallography of [Pt(fdpb)Cl] [Hfdpb = 1,3-Bis(5-trifluoromethyl-2-pyridyl)benzene]

Yuta Nishiuchi,[a] Asuka Takayama,[b] Takayoshi Suzuki,[b] and Kazuteru Shinozaki*[a]

Keywords: Luminescence / Polymorphism / Phase transitions / Stacking interactions / Crystal engineering

We investigated polymorphism in [Pt(fdpb)Cl] [Hfdpb = 1,3-bis(5-trifluoromethyl-2-pyridyl)benzene]. The following polymorphs of the complex were crystallized: yellow [Form Y; orthorhombic, $Pca2_1$, a = 23.4336(14) Å, b = 4.6377(2) Å, c = 15.7845(9) Å, Z = 4], red [Form R; monoclinic, $C2/c$, a = 21.3619(12) Å, b = 13.5629(7) Å, c = 13.6974(6) Å, β = 122.301(2)°, Z = 8], and dark green [Form G; monoclinic, $P2_1/a$, a = 6.7953(4) Å, b = 18.2519(12) Å, c = 13.5199(8) Å, β = 96.039(2)°, Z = 4]. The yellow color of Form Y was due to the influence of stacking on the π,π* absorption of the Pt molecule; the red color of Form R originated from a MMLCT absorption due to Pt–Pt interactions in a closely stacked dimer; and the dark green of Form G was attributed to the absorption of a linear array of Pt^{II} complexes. The polymorphs emitted luminescence at around 550 (Form Y), 670 (Form R), and 750 nm (Form G). Mechanical grinding of the crystals changed the polymorphs from the crystalline to the amorphous phase; the emission spectra of ground samples of Forms Y and R, observed at 750 nm, were identical. When the amorphous solid was heated to around 500 K, the emission spectrum was blueshifted to 670 nm due to a phase transition from amorphous to crystalline. Heating also caused a crystal–crystal transformation; phase transitions from Form G to Form R and Form R to Form Y proceeded at 430–470 and 540–560 K, respectively.

Introduction

Polymorphism in Pt^{II} complexes has been a subject of investigation since 1934, when Morgan and Burstall discovered red and yellow polymorphs of $[Pt(bpy)Cl_2]$ (bpy = 2,2′-bipyridine).[1] X-ray crystallography of the polymorphs revealed the Pt···Pt distance and molecular arrangement in the red and yellow crystals to be quite different.[2–5] Recently, Grzesiak and Matzger reported selective syntheses of polymorphs of $[Pt(bpy)Cl_2]$ and $[Pt(phen)Cl_2]$ by polymer-induced heteronucleation.[6] The yellow color is intrinsic to the monomeric molecule, while the red color arises from Pt–Pt interactions (Pt···Pt distance 3.4 Å) in the linear chain.[7–9] Many Pt^{II} complexes have been found to show dimorphism, which is dependent on the molecular arrangement in the crystal.[10–13] The color of the crystal is easily changed by environmental stimuli such as the application of pressure, exposure to organic solvent vapor, or mechanical grinding. Pressure-induced redshifts of the emission band have been reported for square-planar Pt^{II} complexes.[14–16] For closely stacked complexes, a valence band is generated by the overlap of filled $5d_{z^2}$ orbitals of the Pt centers and a conduction band is created from vacant $6p_z$ orbitals. Because the band gap depends to a large extent on the Pt···Pt distance, the emission energy decreases dramatically with the application of external pressure. The pressure dependence of $[Pt(bpy)Cl_2]$ luminescence has also been reported; a red emission from the ^{3}MLCT (Pt d_{z^2}→bpy π*) state was converted to a yellow emission from the ^{3}LF state.[17] When a crystal of a Pt^{II} complex was exposed to organic solvent vapor, its color and emission color changed from yellow to red.[18,19] This phenomenon was caused by a structural change due to sorption of organic solvent molecules into the crystal lattice; this is classified as pseudo-polymorphism.[20–22] We reported a red emission from a N^C^N cyclometalated complex [Pt(dpb)Cl] [Hdpb = 1,3-bis(2-pyridyl)benzene] in the amorphous phase produced by mechanical grinding of a crystal.[23] Williams et al. attributed the red emission to a ^{3}π,π* transition in the Pt^{II} complex dimer/aggregate.[24,25] They also exploited a combination of the green monomer emission and the red emission in OLED devices.[26,27] We reported the emission properties of an analogous complex, [Pt(5dpb)Cl] [H5dpb = 1,3-bis(5-methyl-2-pyridyl)benzene],[23] which also emitted yellow-green luminescence from the π,π* state in dilute solution. When the solution concentration was increased, the emission color changed to orange as a result of excimer formation. In the solid state, the emission color was yellow due

[a] Department of Chemistry, Graduate School of Nanobiosystem Sciences, Yokohama City University,
22-2 Seto, Yokohama 236-0027, Japan
Fax: +81-45-787-2185
E-mail: shino@yokohama-cu.ac.jp
[b] Department of Chemistry, Faculty of Science, Okayama University,
3-3-1 Tsushimanaka, Okayama 700-8530, Japan

Supporting information for this article is available on the WWW under http://dx.doi.org/10.1002/ejic.201001359.

to π–π stacking with neighboring units.[28] When the crystals were crushed and ground with a pestle and mortar, the color turned to orange, similar to the color of the excimer emission in solution; the fast rise and slow decay of the orange emission were observed by laser photolysis.

In this work, we synthesized a new complex, [Pt(fdpb)-Cl] [Hfdpb = 1,3-bis(5-trifluoromethyl-2-pyridyl)benzene] (Figure 1), which we expected to be color-tunable on the basis of energy changes in the electronic states due to the introduction of a strong electron-withdrawing group. Although the color of the complex in solution was yellow, as are many Pt^{II} complexes, the complex was crystallized as yellow, red, and dark green polymorphs. In this report, the crystal structures of the polymorphs are presented and the origin of the colors is discussed with reference to the crystal structure of each polymorph. We also achieved color changes due to amorphization by mechanical grinding, a crystal–amorphous phase transition upon heating, and crystal–crystal phase transitions in the crystalline polymorphs upon heating.

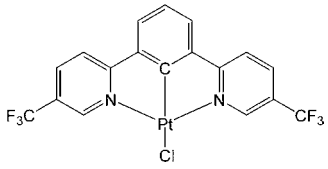

Figure 1. [Pt(fdpb)Cl].

Results and Discussion

Color and Luminescence of the Polymorphs

Slow evaporation of the solvent from a chloroform solution containing [Pt(fdpb)Cl] produced a mixture of yellow, red, and dark green crystals on the sides and bottom of the flask. To obtain each type of crystal selectively, the following procedures were carried out. Yellow crystals (Form Y) were obtained from a DMSO solution by removal of the solvent with a heat gun; red crystals (Form R) were obtained by solvent evaporation at room temperature with a rotary evaporator; and dark green crystals (Form G) were precipitated from a concentrated solution placed in a freezer. When Forms Y and G were immersed in a chloroform solution containing [Pt(fdpb)Cl], they gradually transformed into Form R. It was concluded that these crystals were polymorphs of the Pt^{II} complex crystal.[29] Form R was the most stable form in solution at room temperature, while Forms Y and G seemed to be stable at higher and lower temperatures, respectively. The ^1H NMR [δ = 9.76 (2 H), 8.31 (2 H), 8.10 (2 H), 7.90 (2 H), 7.60 (1 H) ppm], absorption (λ_{abs} = 397 nm, ε = 5280 $M^{-1}cm^{-1}$; λ_{abs} = 495 nm, ε = 4910 $M^{-1}cm^{-1}$) and emission (λ_{em} = 550 nm) spectra of Forms Y, R, and G in chloroform solution were identical. The emission quantum yields and lifetimes in degassed solution were also the same (ϕ = 0.69, τ = 5.8 μs).[30] Figure 2 shows the absorption and emission spectra of [Pt(fdpb)Cl] in chloroform. The absorption band at around 400 nm and the emission peaks were assigned to the π,π* transition, based on literature data. A weak band at 497 nm in the absorption spectrum was attributed to the ^{3}π,π* transition, because the absorption band was a mirror image of the emission spectrum.

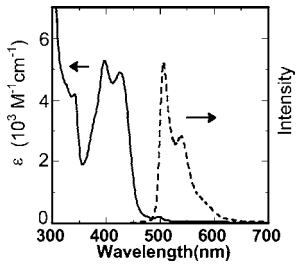

Figure 2. Absorption (solid line) and emission (dashed line) spectra of [Pt(fdpb)Cl] in chloroform. Absorption peaks are observed at 397 (ε = 5280 $M^{-1}cm^{-1}$), 425 (ε = 4910 $M^{-1}cm^{-1}$), and 497 nm (ε = 220 $M^{-1}cm^{-1}$), and emission peaks are observed at 505 and 539 nm.

The absorption spectra of Forms Y, R, and G are shown in Figure 3. For Form Y, absorption bands were observed at 450 and 505 (sh) nm, while for Form R, an absorption edge was observed at 600 nm. Absorption bands having peaks at 500 and 630 nm were observed in the spectrum of Form G. The emission spectra of Forms Y, R, and G are also shown in Figure 3. Although a structured area was observed at around 550 nm in the spectrum of Form Y, the emission peaks of Forms R and G were broad, at 670 and 750 nm, respectively. Based on previous studies of crystals of related Pt^{II} complexes, the emission spectrum of Form Y was attributed to the π,π* transition of the Pt monomer, while the broad peak of Form R was assigned as the emission of a dimer or oligomer. The near-infrared emission of Form G was similar to that obtained in a previous study for a Pt^{II} oligomer in solution.[10]

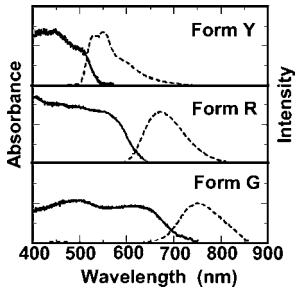

Figure 3. Absorption (solid lines) and emission (dashed lines) spectra of Forms Y, R, and G in the solid state.

Crystal Structure of Form R

The molecular structure of Form R of [Pt(fdpb)Cl] is shown in Figure 4. The Pt^{II} complex is nearly planar and adopts pseudo-C_2 symmetry, with distances of Pt1–C1 1.908(2), Pt1–N1 2.032(2), Pt1–N2 2.034(2), Pt1–Cl1 2.4074(7) Å, and angles of N1–Pt1–Cl1 97.95(6), N2–Pt1–Cl1 100.76(7)° (at 188 K). As seen in Figure 5, the Pt^{II} com-

plexes are aligned in a zigzag fashion with a head-to-tail arrangement, and a side-by-side assembly of this pattern forms a molecular sheet parallel to the (–101) plane of the crystal.[31] The Pt···Pt distance between the nearest neighbors in the zigzag pattern is 9.668 Å, and the Pt···Pt distance between adjacent patterns is 13.520 Å. The crystal of Form R is built up through stacking of molecular sheets, each individual Pt^{II} complex forming a dimer with another complex in an adjacent molecular sheet (stacking type A, circled in Figure 6). Figure 6 also shows stacking type A viewed along the Pt···Pt bond; one molecule is rotated by approximately 120° with respect to the other molecule around the Pt···Pt axis to avoid a like–like interaction. The Pt···Pt distance (*r*) is 3.259 Å (at 188 K); this length, which is appropriate for a metal–metal bond, is shorter than those of the red crystals of $[Pt(bpy)Cl_2]$[7] [3.448(1) Å] and the red crystals of $[Pt(bpy)(CN)_2]$ [3.346(1) Å].[32] Another type of π–π stacking, type B, is also shown in Figure 6. Again, each Pt is paired with a Pt in the adjacent sheet, but here, while the spacing between molecules is approximately 3.5 Å, the Pt···Pt distance is 5.077 Å. The two Pt^{II} complexes in stacking type B are arranged in antiparallel fashion, diminishing their dipole moments of 10.2 Debye, which was predicted by a DFT calculation.[33,34] In stacking type B, with favorable like–unlike interactions, the interaction between overall molecular dipoles is more important than local electrostatic interactions.[35]

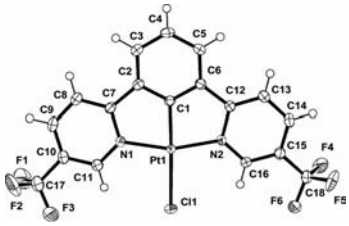

Figure 4. Molecular structure of [Pt(fdpb)Cl] in Form R.

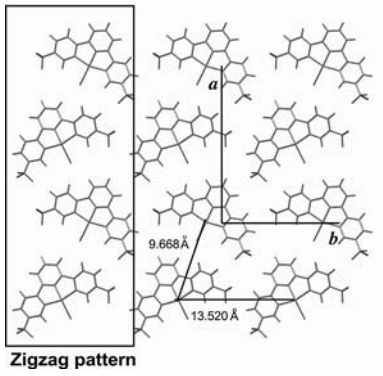

Figure 5. Zigzag patterns and sheet structure of Form R.

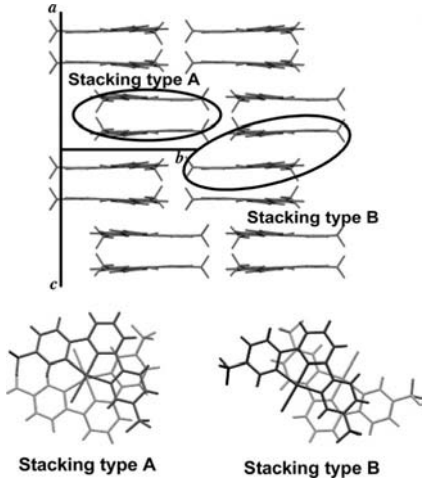

Figure 6. Molecular stacking structures of Form R and binary stacking units (stacking types A and B).

Crystal Structure of Form G

The molecular structure of the Pt^{II} complex in Form G was found to be exactly the same as that in Form R. The distances and angles were evaluated as follows: Pt1–C1 1.903(8), Pt1–N1 2.035(6), Pt1–N2 2.045(6), Pt1–Cl1 2.403(2) Å, N1–Pt1–Cl1 98.6(2), and N2–Pt1–Cl1 100.5(2)°. It also contains the same zigzag pattern and sheet consisting of Pt^{II} complexes (shown in Figure 7). The Pt···Pt distance between nearest molecules in the pattern is 9.650 Å, while the Pt···Pt distance between adjacent patterns is 13.563 Å. These results are similar to those for Form R; however, the assembly of the molecular sheets is quite different. When viewed along the *b* axis (Figure 8), the sheet-stacking structure and 1D-columnar structure of Form G may be clearly seen. Form G has a single stacking manner (stacking type C in Figure 8), with successive molecules rotated approximately 120° around the stacking axis and a Pt···Pt distance of 3.437 Å. Stacking type C contains molecules that are mutually stacked to avoid like–like interactions but with favorable Pt–Pt interactions in the stacked pair. Although the dipole moment of each molecule is not cancelled by the dipole of the adjoining molecule, the overall dipole moment of the stack in type C is cancelled by that of an adjacent stack. The Pt atoms in the 1D column are aligned in a straight fashion, with a Pt···Pt···Pt angle of 162.7°. The columnar structure is similar to the aggregation structure of a similar complex, [Pt(tpy)(C≡C–C≡CH)]OTf (tpy = 2,2′:6′,2′′-terpyridine), which has a dark green color in the solid state.[10]

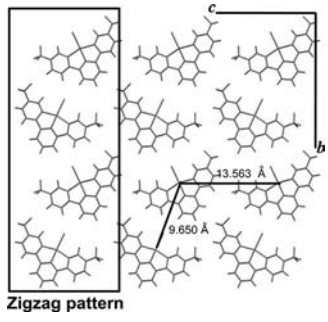

Figure 7. Zigzag patterns and sheet structure of Form G.

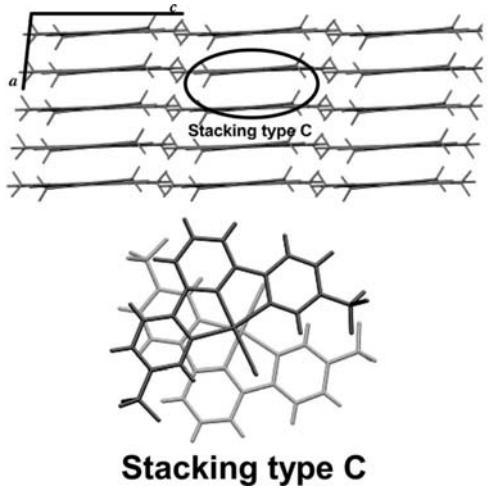

Figure 8. Stacking structure of Form G when viewed along the *b* axis of the crystal and stacking type C shown along the *a* axis.

Crystal Structure of Form Y

Although the molecular structure of Form Y [distances and angles: Pt1–C1 1.898(6), Pt1–N1 2.027(4), Pt1–N2 2.031(4), Pt1–Cl1 2.3860(18) Å, N1–Pt1–Cl1 98.23(14), and N2–Pt1–Cl1 100.73(14)°] is similar to those of Forms R and G, the molecular arrangement in the crystal is different. When viewed along the *b* axis (Figure 9), a molecular sheet composed of Pt^{II} complex zigzag patterns is seen, as in Forms R and G. The Pt···Pt distances between nearest neighbors are 8.279 and 11.847 Å. However, the molecular planes are not parallel to the (010) plane of the crystal; instead, they are tilted by approximately 30°. As shown in Figure 10, successive molecules accumulate in a uniform way and build up a 1D column parallel to the *b* axis. The Pt···Pt distance between nearest neighbors in the 1D column is 4.638 Å, which is too far for interaction via overlapping Pt d_{z^2} orbitals. To avoid like–like interactions, the molecules are slightly offset with respect to each other (stacking type D, as shown in Figure 10); however, the dipole moment of each molecule is not cancelled by that of an adjacent molecule. Therefore, the 1D column retains some polarization when the individual molecular dipole moments are taken together, and, consequently, the whole crystal shows some polarization parallel to the *c* axis. The crystal seems not to obey the close packing rule.[35]

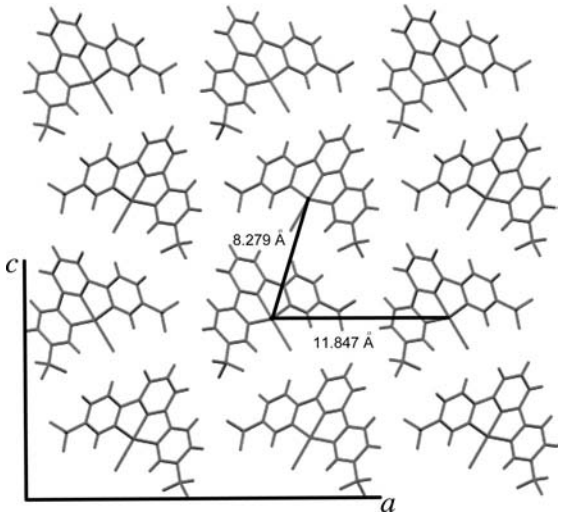

Figure 9. A view along the *b* axis of Form Y.

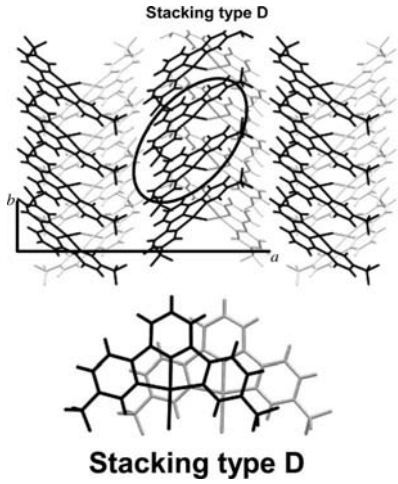

Figure 10. 1D column structure of Form Y viewed along the *c* axis and stacking type D.

Emissions of the Discrete Molecule

Although [Pt(fdpb)Cl] emitted green luminescence in solution, the crystals emitted in the yellow, red, or near-infrared regions, depending on the crystal structure. The color variety results from the difference in molecular stacking type, as clarified by X-ray crystallography. Green luminescence from the Pt-based molecule was also observed in a thin film deposited on a glass substrate by physical vapor deposition. When intermolecular interactions such as π–π or Pt–Pt interactions are weak, the color of the luminescence is likely to be green even in the solid state. However, the emission profile of the thin film was slightly different from that of the solution, as shown in Figure 11. The emission spectra $I(\tilde{\nu})$ were simulated by Equation (1).[36,37]

$$I(\tilde{\nu}) = \sum_{\nu_M=0}^{5}\sum_{\nu_L=0}^{5}\left(\frac{E_0 - \nu_M\hbar\omega_M - \nu_L\hbar\omega_L}{E_0}\right)^3\left(\frac{S_M{}^{\nu_M}}{\nu_M!}\right)\left(\frac{S_L{}^{\nu_L}}{\nu_L!}\right) \exp\left\{-4\ln 2\left(\frac{\tilde{\nu} - E_0 + \nu_M\hbar\omega_M + \nu_L\hbar\omega_L}{\Delta\tilde{\nu}_{1/2}}\right)^2\right\} \quad (1)$$

where S_M and S_L are Huang–Rhys factors for medium- and low-frequency modes, with $\hbar\omega_M$ and $\hbar\omega_L$, respectively; E_0 is the 0–0 band energy of the emission spectrum; and $\Delta\tilde{\nu}_{1/2}$ is the FWHM (full-width half maximum) of the vibronic band. Spectral fittings with the parameters E_0 = 19270 cm^{-1}, $\hbar\omega_M$ = 1330 cm^{-1}, S_M = 0.58, $\hbar\omega_L$ = 730 cm^{-1}, S_L = 0.63, $\Delta\tilde{\nu}_{1/2}$ = 750 cm^{-1} for the thin film and E_0 = 19750 cm^{-1}, $\hbar\omega_M$ = 1290 cm^{-1}, S_M = 0.53, $\hbar\omega_L$ = 630 cm^{-1}, S_L = 0.56, $\Delta\tilde{\nu}_{1/2}$ = 710 cm^{-1} for the solution are in good

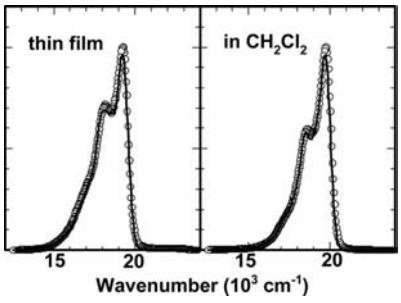

Figure 11. Emission spectra (circles) and spectral fitting curves (solid lines) for [Pt(fdpb)Cl] in thin film and in solution.

agreement with the observed spectra. Although the value of E_0 for the thin film is smaller than that for the solution, due to interaction with the glass substrate, the other parameters are nearly the same.

DFT calculations showed that the lowest electronic transition of [Pt(fdpb)Cl] is the π,π* transition, polarized to the long axis of the fdpb ligand plane (*x* axis); the HOMO is a π orbital mainly consisting of the Pt d_{yz}, Cl p_z, and phenyl π orbitals, and the LUMO is a π* orbital delocalized on the fdpb ligand (see Supporting Information).[38] The energies of the HOMO and LUMO were predicted to be –6.15 and –2.91 eV, respectively. The HOMO–1 (–6.55 eV) is the p_x orbital of Cl and the HOMO–2 (–6.93 eV) is the almost filled Pt $5d_{z^2}$ orbital. The LUMO+1 (–2.83 eV) and the LUMO+2 (–2.03 eV) are π* orbitals delocalized on the fdpb ligand. The LUMO+4, consisting of vacant Pt p_z and d_{z^2} orbitals, is much higher in energy (–0.71 eV) than the π* orbitals. The HOMO–2→LUMO transition, which is a Pt-to-fdpb charge transfer (MLCT) transition, is *z*-polarized. Since these results are very similar to those obtained for $[Pt(bpy)Cl_2]$,[5,39] the assignments for the electronic transition of $[Pt(bpy)Cl_2]$ polymorphs were applied in this case. When the [Pt(fdpb)Cl] molecules stack with each other to form stacking types A–D, the HOMO–LUMO energy gap decreases relative to that of the monomer.

Emissions of Form Y

For stacking type D, forming a weakly stacked pair with almost C_2 symmetry, the overlap of the monomer π and π* orbitals slightly stabilizes the LUMO and destabilizes the HOMO in energy. However, the bonding and antibonding orbitals arising from the filled Pt $5d_{z^2}$ orbitals have almost the same energy, because the Pt–Pt interaction is very weak. Therefore, the HOMO and LUMO of stacking type D with C_2 symmetry still has the π and π* characteristics of the monomer, and the observed emission spectrum has a similar profile to the π,π* transition of the monomer. Figure 12 shows the emission spectrum of Form Y at 180 K. The spectrum was simulated by spectral fitting using Equation (1), and the simulation (solid line) is in good agreement with the experimental result (circles). The evaluated parameters are E_0 = 18980 cm^{-1}, $\hbar\omega_M$ = 1260 cm^{-1}, S_M = 0.33, $\hbar\omega_L$ = 930 cm^{-1}, S_L = 1.57, and $\Delta\tilde{\nu}_{1/2}$ = 920 cm^{-1}. The 0–0 band energy of E_0 is lower than that of the thin film or the solution, which is consistent with the above argument that the HOMO–LUMO energy gap in stacking type D is smaller than that of the monomer. The values of $\hbar\omega_M$ and $\hbar\omega_L$ are almost the same as those of the monomer. Therefore, the transition is suggested to be the π,π* transition. The S_M and S_L values, which represent the displacement in equilibrium structure between the excited and ground-state molecules, are smaller and larger, respectively, than those of the monomer. When the temperature was raised from 180 to 410 K, the emission spectrum became sharp. The emission parameters are E_0 = 18950 cm^{-1}, $\hbar\omega_M$ = 1300 cm^{-1}, S_M = 0.17, $\hbar\omega_L$ = 850 cm^{-1}, S_L = 2.41, and $\Delta\tilde{\nu}_{1/2}$ = 950 cm^{-1} at 296 K, and E_0 = 18980 cm^{-1}, $\hbar\omega_M$ = 1160 cm^{-1}, S_M = 0.14, $\hbar\omega_L$ = 830 cm^{-1}, S_L = 2.55, and $\Delta\tilde{\nu}_{1/2}$ = 980 cm^{-1} at 410 K. The 0–0 band energy E_0 is independent of temperature. The sharpening of the spectrum with increasing temperature is attributed to the decrease in the value of S_M.

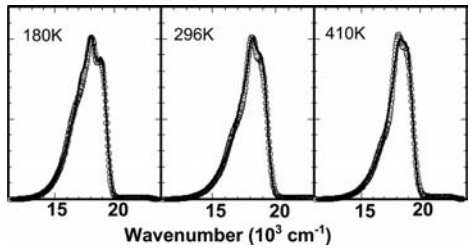

Figure 12. Emission spectra (circles) and simulations (solid lines) of Form Y at 180, 296, and 410 K.

Emission of Form R

For Form R, which has a dimer structure (stacking type A) with a strong Pt–Pt interaction, the HOMO switches from the ligand π orbital to the dσ* orbital produced by overlapping Pt $5d_{z^2}$ orbitals, by analogy with Miskowsky's work.[39] The broad emission at 670 nm was assigned to the dσ*→π* (MMLCT) transition, which depends strongly on the Pt···Pt distance. X-ray crystallography of Form R at various temperatures reveals an explicit relationship between distance (*r*) and temperature: *r* = 3.306 Å at 293 K, 3.259 Å at 188 K, and 3.229 Å at 113 K. As shown in Table 1, the crystals show *C*2/*c* symmetry, and both the *a* and *c* axes of the crystal diminish with decreasing temperature. Thus, the crystal density of Form R decreases as the temperature is raised. The relationship between Pt···Pt distance and temperature (*T*) is expressed by Equation (2).[7]

$$r = 3.20 + 0.00029T + 3.47 \times 10^{-7}T^2 \quad (2)$$

where *r* values are the Pt–Pt distances in Form R obtained by X-ray crystallography. It was found that, when the Pt···Pt bond shrinks due to decreasing temperature, the ^{3}MMLCT emission energy decreases due to destabilization of the dσ* orbital.

Figure 13 shows emission spectra of Form R obtained at various temperatures from 500 to 80 K. As the crystal is cooled from room temperature, the spectrum is redshifted from 670 to 710 nm; as the temperature is raised to 500 K, the spectrum is blueshifted to 650 nm. By estimating the Pt···Pt distance (r) corresponding to each temperature (T) from Equation (2), we obtained a relationship between the ^{3}MMLCT energy ($\tilde{\nu}_{max}$) and r, according to the literature.[7] A plot of $\tilde{\nu}_{max}$ (in cm^{-1}) against r^{-3} gives a good linear correlation, which is similar to that obtained for [Pt(bpy)Cl$_2$].[7] This relationship is expressed by Equation (3).

$$\tilde{\nu}_{max} = 23.9 \times 10^3 - 3.28 \times 10^5 r^{-3} \quad (3)$$

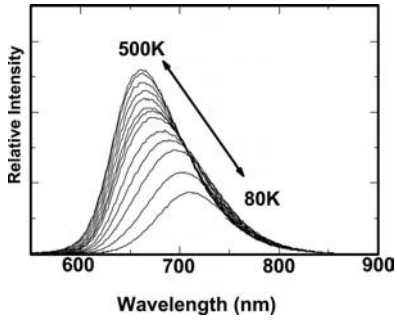

Figure 13. Emission spectra of Form R at various temperatures (500, 480, 440, 400, 360, 320, 300, 280, 240, 200, 160, 120, and 80 K).

The value of 23.9×10^3 cm^{-1} should be the ^{3}MLCT (Pt d_{z^2}→fdpb π*) energy of a pair with infinite Pt···Pt distance, which is identical to that of the monomer.[7] The $\tilde{\nu}_{max}$ = of the monomer could not be estimated from the emission and absorption spectra because of interference from a strong π,π* emission and an intense absorption at around 400 nm.

Emissions of Form G

The green color of Form G results from Pt–Pt interactions in a linear Pt chain, similar to those in Magnus' green salt.[40] Even for such a Pt–Pt linear chain, MO treatment of a Pt–Pt dimer was still applicable to spectral analysis.[39] The emission of Form G was therefore assigned as a MMLCT emission, similarly to that in Form R. However, the emission peak wavelength of Form G at room temperature is 750 nm, which is lower in energy than that of the Pt–Pt dimer of Form R, despite the fact that the Pt···Pt distance of r = 3.4 Å at 188 K is greater than that of the dimer in Form R. If the discrete energy level of the HOMO could be replaced by bands composed of filled Pt d_{z^2} orbitals in the Pt–Pt linear chain, the excitation energy would be decreased to a greater extent than that of the dimer/aggregate.[41] Figure 14 shows emission spectra of Form G obtained at various temperatures. As the temperature is raised from 100 to 280 K, the emission spectrum is blueshifted and the intensity increases. By analogy to the results obtained for Form R, the Pt···Pt distance in the linear chain was concluded to have been elongated by the increase in temperature.

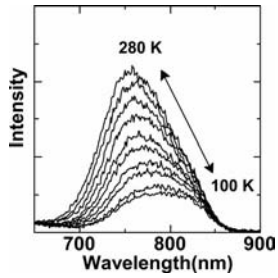

Figure 14. Emission spectra of Form G at various temperatures (280, 260, 240, 220, 200, 180, 160, 140, 120, and 100 K).

Mechanochromism of the Polymorphs

When the crystals were crushed and ground with a pestle and mortar, the color of Form Y changed from yellow to dark red, as did [Pt(dpb)Cl].[23] Form R also turned dark red. Powder X-ray diffraction (XRD) indicates that the ground samples of Forms Y and R are almost amorphous, because their diffraction patterns become broader and weaker (see Supporting Information).[23] The color of luminescence from the compounds is also changed by grinding, as shown in Figure 15; the two ground samples emit identical dark red signals at around 750 nm at room temperature. It was concluded that the Pt–Pt interactions and/or π–π interactions were very similar in both of the ground samples and were independent of those in the original crystal form. Assuming that the dark red emission in the amorphous phase is predominantly due to the ^{3}MMLCT state of the dimer or aggregate, r was evaluated as 3.14 Å by using the relationship between $\tilde{\nu}_{max}$ = and r^{-3}. The r value can be considered to be the average Pt···Pt distance in an amorphous phase with a random and nonperiodic structure. The average distance r is shorter than that in the linear chain in Form G (r = 3.437 Å at 188 K) and the dimer of Form R (r = 3.259 Å at 188 K). Wenger et al. demonstrated the conversion from a red form of [Pt(bpy)Cl$_2$] to a yellow form under the application of hydrostatic pressure.[17] In this case, the red form (r = 3.45 Å and ρ = 2.55 g cm^{-3}) was transformed to the yellow form (r = 3.25 Å and ρ =

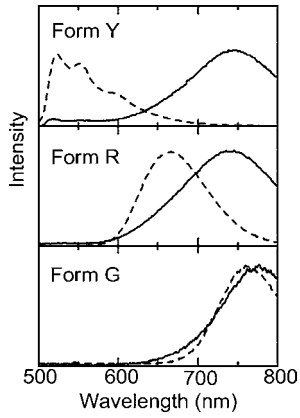

Figure 15. Emission spectra of Forms Y, R, and G at room temperature. Dashed and solid lines represent the emission spectra of crystalline and ground samples, respectively.

2.65 g cm^{-3}) under 17 kbar pressure. The phase transition proceeded with an increase in crystal density when pressure was applied to the crystal. By analogy with this pressure effect, the density of the amorphous phase was concluded to be greater than that of Form R. When Form G was ground to a fine powder, XRD analysis gave a broad and weak pattern indicating amorphization (see Supporting Information). As seen in Figure 15, however, an emission was still observed at around 750 nm, which was nearly the same as that of crystalline Form G.

Phase Transitions of the Polymorphs

The crystal densities (ρ, g cm^{-3}) at 185–188 K, obtained by X-ray crystallography, were in the order 2.381 (Form G) > 2.367 (Form R) > 2.315 (Form Y), as shown in Table 1. The density of Form R was found to depend on the temperature: 2.382 at 113 K, 2.367 at 188 K, and 2.323 g cm^{-3} at 293 K. As the temperature was raised, the density of Form R seemed to approach that of Form Y. When Form R was heated to around 550 K in a sealed glass tube purged with Ar gas, the red color changed to yellow. This irreversible phase transition from Form R to Form Y was nearly a single-crystal–single-crystal phase transition. As shown in Figure 16, differential scanning calorimetry (DSC) showed a negative peak, indicating a phase transition at 274.6–287.2 °C (548–560 K). When the temperature was raised, the thermodynamically stable form converted to another low-density form, increasing the entropy of the crystal. This is in agreement with the principle of close packing;[42] a transformation to a less dense form occurred to avoid an increase in the void space of the crystal. The increase in the enthalpy term ΔH as a result of the increase in temperature was compensated by the increase in the positive entropy term $T\Delta S$.[35] A similar free energy compensation for red–yellow transformations of [Pt(bpy)Cl$_2$] dimorphs was reported by Grzeiak and Matzger.[6] Form G was also transformed to Form R by heating; when Form G was heated to around 500 K, the color of the crystal changed to red. A blueshift from 750 to 670 nm was observed in the emission spectrum at room temperature. The transformation from Form G to Form R was also irreversible and proceeded in accordance with the principle of close packing. Further heating caused a second phase transition from the red form to the yellow form. The DSC trace of Form G is shown in Figure 16. The first and second phase transitions were observed at 156.8–194.4 °C (430–468 K) and 266.4–283.8 °C (540–557 K). When the ground sample in the amorphous phase was heated to around 500 K under an Ar atmosphere, the color changed to red and a bright red emission appeared. The emission spectrum of this material at room temperature was identical to that of Form R, with a peak at 670 nm. It was concluded that the amorphous-phase molecule crystallized with heating. By analogy with the free energy compensation argument, the enthalpy change in the amorphous phase due to heating was compensated by the increase in entropy due to the phase transition to a low-density crystal.

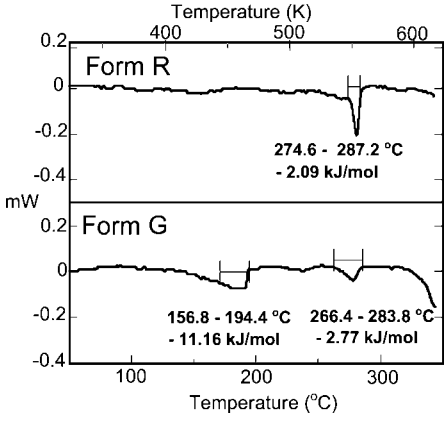

Figure 16. DSC traces for Forms R and G.

The phase transition is summarized in Scheme 1. Heating causes irreversible crystal–crystal phase transitions from Form G through Form R to Form Y, and sublimation of [Pt(fdpb)Cl] takes place when the temperature exceeds 570 K. The crystalline polymorphs are converted into the amorphous phase by mechanical grinding, while the amorphous solid is converted to Form R when heated to around 500 K. The red and yellow polymorphs of [Pt(fdpb)Cl] in the Form-R–Form-Y–amorphous transformation cycle may be easily produced by a combination of heating and grinding.

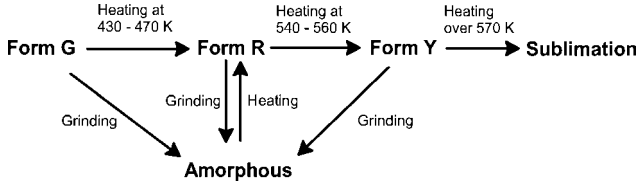

Scheme 1. Phase transition diagram for [Pt(fdpb)Cl].

Conclusions

We present a variety of solid-state polymorphs of [Pt(fdpb)Cl], which show various emissions: a green emission from a thin film deposited on a substrate by physical vapor deposition, a yellow emission from Form Y, a red emission from Form R, a dark red emission from the ground solid in the amorphous phase, and a near-infrared emission from Form G. These multicolored emissions result from the tuning of the HOMO–LUMO energy gap due to differences in the Pt–Pt and π–π interactions between molecules in the solid state. In Form Y, [Pt(fdpb)Cl] emits yellow luminescence from the $^3\pi,\pi^*$ excited state, stabilized by the π–π interaction between Pt^{II} complexes in a 1D column. The red emission of Form R was attributed to phosphorescence from the ^{3}MMLCT state of the Pt–Pt dimer. The linear chain of Pt^{II} complexes in Form G emits luminescence with ^{3}MMLCT character. The polymorphs are easily interconverted by a combination of heating and grinding.

Table 1. Crystallographic information for Forms Y, R, and G of [Pt(fdpb)Cl].

	Form Y	Form R-1	Form R-2	Form R-3	Form G
Color	Yellow	Red	Red	Red	Dark green
Crystal system	orthorhombic	monoclinic	monoclinic	monoclinic	monoclinic
Space group	$Pca2_1$	$C2/c$	$C2/c$	$C2/c$	$P2_1/a$
Temperature (K)	185(2)	113(2)	188(2)	293(2)	188(2)
a (Å)	23.4336(14)	21.3256(5)	21.3619(12)	21.5196(5)	6.7953(4)
b (Å)	4.6377(2)	13.5733(4)	13.5629(7)	13.5787(7)	18.2519(12)
c (Å)	15.7845(9)	13.5812(4)	13.6974(6)	13.8711(3)	13.5199(8)
α (°)	90	90	90	90	90
β (°)	90	121.999(1)	122.301(2)	122.492(1)	96.039(2)
γ (°)	90	90	90	90	90
Z	4	8	8	8	4
V (Å^3)	1715.42(16)	3333.87(16)	3354.4(3)	3418.8(2)	1667.52(17)
ρ (g cm^{-3})	2.315	2.382	2.367	2.323	2.381
$R1$[a]	0.0309	0.0281	0.0198	0.0262	0.0454
$wR2$[b]	0.0581	0.0706	0.0474	0.0589	0.1187

[a] $R1 = \Sigma||F_o| - |F_c||/\Sigma|F_o|$. [b] $wR2 = [\Sigma w(F_o^2 - F_c^2)^2/\Sigma wF_o^2]^{1/2}$.

These advantages of [Pt(fdpb)Cl] may be useful in the development of multicolored, color-tunable luminescent devices.

Experimental Section

Hfdpb: The ligand was synthesized from 1,3-benzenediboronic acid (193.4 mg), 2-chloro-5-(trifluoromethyl)pyridine (535.7 mg), and tetrakis(triphenylphosphane)palladium(0) (269.5 mg) by heating at reflux in an aqueous sodium carbonate solution (3.2%, 30 mL) and benzene (30 mL) mixture for 7 d. The desired ligand was extracted with chloroform from the resulting solution and purified by silica gel column chromatography with hexane/ethyl acetate (7:1) as an eluent. White crystals of the ligand were obtained in 21.4% yield. ^{1}H NMR (300 MHz, $CDCl_3$, 298 K): δ = 9.00 (s, 2 H, CH), 8.80 (s, 1 H, CH), 8.18 (dd, J_{HH} = 1.8, 7.8 Hz, 2 H, CH), 8.06 (dd, J_{HH} = 2.1, 8.7 Hz, 2 H, CH), 8.04 (d, J_{HH} = 8.1 Hz, 2 H, CH), 7.68 (t, J_{HH} = 7.5 Hz, 1 H, CH) ppm. APCI-MS: m/z = 369 $[M + H]^+$.

[Pt(fbpb)Cl]: The complex was obtained by heating Hfdpb (92.1 mg) and potassium tetrachloroplatinate(II) in acetic acid (70 mL) at reflux for 2 d. After the removal of acetic acid from the reaction mixture, water/dichloromethane mixture was added to the residual material. The Pt^{II} complex, which was extracted in dichloromethane, was purified by passing it through a silica gel column and recrystallized from chloroform (yield 13.8%). ^{1}H NMR (300 MHz, $CDCl_3$, 298 K): δ = 9.76 (s, 2 H, CH), 8.31 (d, J_{HH} = 8.9 Hz, 2 H, CH), 8.10 (d, J_{HH} = 7.8 Hz, 2 H, CH), 7.90 (d, J_{HH} = 7.8 Hz, 2 H, CH), 7.60 (t, J_{HH} = 8.1 Hz, 1 H, CH) ppm. ESI-MS: m/z = 562 $[(M - Cl)]^+$, 603 $[(M - Cl + CH_3CN)]^+$. [Pt(fdpb)-Cl] crystallized in polymorphs, which were yellow, red, and dark-green crystals. The red and dark-green single crystals suitable for X-ray crystallography were picked up from crystals obtained by a slow evaporation of solvent from a chloroform solution. Yellow single crystals were prepared by physical vapor deposition. The red crystals were placed in a vacuum glass tube and heated at 560–590 K with a temperature gradient.

Crystallographic Studies: For the measurement at temperatures below 200 K, a suitable crystal mounted with a cryoloop and Paratone-N was flash-cooled by a cold nitrogen stream. For the measurement at room temperature, a crystal was glued on top of a glass capillary with epoxy. The X-ray diffraction data were obtained by means of a Rigaku R-axis rapid imaging plate detector with graphite-monochromated Mo-K_α radiation (λ = 0.71073 Å). Data were processed by the Process-Auto program package,[43] and absorption corrections were applied by the numerical method.[44] The structures were solved by the direct method using SIR2004[45] and refined on F^2 (with all independent reflections) with the SHELXL97 program.[46] All non-H atoms were refined anisotropically, and H atoms were introduced at the positions calculated theoretically and treated with riding models. All calculations were carried out by using the CrystalStructure software package.[47] Crystallographic data for the polymorphs are listed in Table 1. CCDC-802103 (Form Y), -802104 (Form G), -802105 (Form R-3), -802106 (Form R-2), and -802107 (Form R-1) contain the supplementary crystallographic data for this paper. These data can be obtained free of charge from The Cambridge Crystallographic Data Centre via www.ccdc.cam.ac.uk/data_request/cif.

Measurements: UV/Vis absorption spectra were measured by a Shimadzu Multispec 1500 spectrometer. A Hamamatsu PMA-10 was used as a photodetector for the solid-state absorption measurements. Luminescence spectra were recorded with a JASCO F-6500 spectrofluorometer. ^{1}H NMR spectra and ESI-MS data were obtained with a JEOL 270 spectrometer and Shimadzu QP-8000 instrument, respectively. The lifetime was evaluated by a least-squares method on a PC for time courses of luminescence recorded by a SONY Tektronix TDS320 digital oscilloscope after a pulse excitation with a Continuum I Nd:YAG laser (355 nm). XRDs were obtained by using a Cu-$K_{\alpha 1}$ line on a RIGAKU RINT 1100 X-ray diffractometer. DSCs were measured with a Shimadzu DSC-60 instrument.

Supporting Information (see footnote on the first page of this article): Geometry of [Pt(fdpb)Cl] for a DFT calculation, HOMOs and LUMOs of [Pt(fdpb)Cl], XRD patterns for Forms Y, R, and G before and after grinding.

Acknowledgments

This work was financially supported by the Japanese Ministry of Education, Science, Sports, and Culture for a Grant-in-Aid for Scientific Research (Grant 17550063) and Yokohama City University (Grants K18034 and K18002).

[1] G. T. Morgan, F. H. Burstall, *J. Chem. Soc.* **1934**, 965–971.
[2] R. S. Osborn, D. Rogers, *J. Chem. Soc., Dalton Trans.* **1974**, 1002–1004.
[3] A. J. Canty, B. W. Skelton, P. R. Trail, A. H. White, *Aust. J. Chem.* **1992**, *45*, 417–423.

[4] R. H. Herber, M. Croft, M. J. Coyer, B. Bilash, A. Sahiner, *Inorg. Chem.* **1994**, *33*, 2422–2426.
[5] W. B. Connick, R. E. Marsh, W. P. Schaefer, H. B. Gray, *Inorg. Chem.* **1997**, *36*, 913–922.
[6] A. L. Grzesiak, A. J. Matzger, *Inorg. Chem.* **2007**, *46*, 453–457.
[7] W. B. Connick, L. M. Henling, R. E. Marsh, H. B. Gray, *Inorg. Chem.* **1996**, *35*, 6261–6265.
[8] V. M. Miskowski, V. H. Houlding, *Inorg. Chem.* **1989**, *28*, 1529–1533.
[9] V. H. Houlding, V. M. Miskowski, *Coord. Chem. Rev.* **1991**, *111*, 145–152.
[10] V. W.-W. Yam, K. M.-C. Wong, N. Zhu, *J. Am. Chem. Soc.* **2002**, *124*, 6506–6507.
[11] X.-Y. Zhou, N. M. Kostić, *Inorg. Chem.* **1988**, *27*, 4402–4408.
[12] A. Şengül, *Turk. J. Chem.* **2004**, *28*, 667–672.
[13] R. D. Gillard, A. Şengül, *Transition Met. Chem.* **2001**, *26*, 339–344.
[14] A. Lechner, G. Gliemann, *J. Am. Chem. Soc.* **1989**, *111*, 7469–7475.
[15] E. Leyrer, F. Zimmermann, J. I. Zink, G. Gliemann, *Inorg. Chem.* **1985**, *24*, 102–106.
[16] G. Levasseur-Thériault, C. Reber, C. Aronica, D. Luneau, *Inorg. Chem.* **2006**, *45*, 2379–2381.
[17] O. S. Wenger, S. García-Revilla, H. U. Güdel, H. B. Gray, R. Valiente, *Chem. Phys. Lett.* **2004**, *384*, 190–192.
[18] M. Kato, A. Omura, A. Toshikawa, S. Kishi, Y. Sugimoto, *Angew. Chem.* **2002**, *114*, 3315; *Angew. Chem. Int. Ed.* **2002**, *41*, 3183–3185.
[19] L. J. Grove, J. M. Rennekamp, H. Jude, W. B. Connick, *J. Am. Chem. Soc.* **2004**, *126*, 1594–1595.
[20] C. E. Buss, K. R. Mann, *J. Am. Chem. Soc.* **2002**, *124*, 1031–1039.
[21] S. M. Drew, D. E. Janzen, C. E. Buss, D. I. MacEwan, K. M. Dublin, K. R. Mann, *J. Am. Chem. Soc.* **2001**, *123*, 8414–8415.
[22] J. W. Grate, L. K. Moore, D. E. Janzen, D. J. Veltkamp, S. Kaganove, S. M. Drew, K. R. Mann, *Chem. Mater.* **2002**, *14*, 1058–1066.
[23] T. Abe, T. Itakura, N. Ikeda, K. Shinozaki, *Dalton Trans.* **2009**, 711–715.
[24] J. A. G. Williams, A. Beeby, E. S. Davis, J. A. Weinstein, C. Wilson, *Inorg. Chem.* **2003**, *42*, 8609–8611.
[25] S. J. Farley, D. L. Rochester, A. L. Thompson, J. A. K. Howard, J. A. G. Williams, *Inorg. Chem.* **2005**, *44*, 9690–9703.
[26] J. Kalinowski, M. Cocchi, D. Virgili, V. Fattori, J. A. G. Williams, *Adv. Mater.* **2007**, *19*, 4000–4005.
[27] M. Cocchi, D. Virgili, V. Fattori, D. L. Rochester, J. A. G. Williams, *Adv. Funct. Mater.* **2007**, *17*, 285–289.
[28] T. Abe, K. Shinozaki, N. Ikeda, T. Suzuki, *Acta Crystallogr., Sect. C* **2007**, *63*, m456–m458.
[29] J. Bernstein, *Polymorphism in Molecular Crystals*, Clarendon Press, Oxford, **2002**.
[30] The values are for infinitely diluted solutions, as the emission quantum yield and lifetime depend on the concentration of [Pt(fdpb)Cl] because of self-quenching or excimer formation.
[31] The same sheet and stacking structures were observed for the [Pt(5dpb)Cl] crystal reported in ref.[28] previously.
[32] W. B. Connick, L. M. Henling, R. E. Marsh, *Acta Crystallogr., Sect. B* **1996**, *52*, 817–822.
[33] Dipole moments of Pt^{II} complexes were calculated at the B3LYP/LanL2DZ for Pt and B3LYP/6-31G* for Cl, C, N, H, F atoms. In the calculation, the average bond lengths and angles determined by the X-ray crystallography were used as data for the geometry of the complex. The dipole moment is larger than those of [Pt(dpb)Cl] (6.3 Debye) and [Pt(5dpb)Cl] (6.1 Debye), because of the strongly electron-withdrawing groups CF_3.
[34] M. J. Frisch, G. W. Trucks, H. B. Schlegel, G. E. Scuseria, M. A. Robb, J. R. Cheeseman, J. A. Montgomery Jr., T. Vreven, K. N. Kudin, J. C. Burant, J. M. Millam, S. S. Iyengar, J. Tomasi, V. Barone, B. Mennucci, M. Cossi, G. Scalmani, N. Rega, G. A. Petersson, H. Nakatsuji, M. Hada, M. Ehara, K. Toyota, R. Fukuda, J. Hasegawa, M. Ishida, T. Nakajima, Y. Honda, O. Kitao, H. Nakai, M. Klene, X. Li, J. E. Knox, H. P. Hratchian, J. B. Cross, C. Adamo, J. Jaramillo, R. Gomperts, R. E. Stratmann, O. Yazyev, A. J. Austin, R. Cammi, C. Pomelli, J. W. Ochterski, P. Y. Ayala, K. Morokuma, G. A. Voth, P. Salvador, J. J. Dannenberg, V. G. Zakrzewski, S. Dapprich, A. D. Daniels, M. C. Strain, O. Farkas, D. K. Malick, A. D. Rabuck, K. Raghavachari, J. B. Foresman, J. V. Ortiz, Q. Cui, A. G. Baboul, S. Clifford, J. Cioslowski, B. B. Stefanov, G. Liu, A. Liashenko, P. Piskorz, I. Komaromi, R. L. Martin, D. J. Fox, T. Keith, M. A. Al-Laham, C. Y. Peng, A. Nanayakkara, M. Challacombe, P. M. W. Gill, B. Johnson, W. Chen, M. W. Wong, C. Gonzalez, J. A. Pople, *Gaussian*, Gaussian, Inc., Wallingford, CT, **2004**.
[35] C. P. Brock, J. D. Dunitz, *Chem. Mater.* **1994**, *6*, 1118–1127.
[36] K. Shinozaki, T. Shinoyama, *Chem. Phys. Lett.* **2006**, *417*, 111–115.
[37] J. V. Casper, T. D. Westmoreland, G. H. Allen, P. G. Bradley, T. J. Meyer, W. H. Woodruff, *J. Am. Chem. Soc.* **1984**, *106*, 3492–3500.
[38] The molecular symmetry is C_{2v}; the molecular plane is set on the *xy* plane and the *y* axis is the Pt–Cl bonding axis.
[39] V. M. Miskowski, V. H. Houlding, *Inorg. Chem.* **1991**, *30*, 4446–4452.
[40] G. Magnus, *Pogg. Ann.* **1828**, *14*, 239–242.
[41] Y.-H. Chen, J. W. Merkert, Z. Murataza, C. Woods, D. P. Rillema, *Inorg. Chim. Acta* **1995**, *240*, 41–47.
[42] A. I. Kitaigorodskii, *Organic Chemical Crystallography*, Consultant's Bureau, New York, **1961**.
[43] Rigaku Corporation, *PROCESS-AUTO*. Automatic Data Acquisition and Processing Package for Imaging Plate Diffractometer, Tokyo, Japan, **1998**.
[44] T. Higashi, *Shape, Program for Absorption*, Rigaku Corporation, Tokyo, Japan, **1999**.
[45] M. C. Burla, R. Caliandro, M. Camalli, B. Carrozzini, G. L. Cascarano, L. De Caro, C. Giacovazzo, G. Polidori, R. Apagna, *J. Appl. Crystallogr.* **2005**, *38*, 381–388.
[46] G. M. Scheldrick, *Acta Crystallogr., Sect. A* **2008**, *64*, 112–122.
[47] Rigaku and Rigaku/MSC, *CrystalStructure, Crystal structure analysis package, ver. 3.7.0*, The Woodlands, TX, USA, **2000**–2005.

Received: December 28, 2010
Published Online: February 23, 2011

